A Model-Based Observer for State and Stress Estimation in Structural and Mechanical Systems: Experimental Validation

Kalil Erazo[a], Eric M. Hernandez[a,*]

[a]*School of Engineering, College of Engineering and Mathematical Sciences, University of Vermont, 33 Colchester Ave. 301 Votey Hall. ,VT, USA*

Abstract

In this paper we present the results from a validation study of a recently proposed model-based state observer for structural and mechanical systems. The observer uses a finite element model of the structure and noise contaminated measurements to estimate the state and stress time histories at arbitrary locations in the structure of interest. The initial conditions and unknown excitations are described by random vectors and random processes with known covariance and power spectral density. A laboratory model consisting of an aluminum cantilever beam was used to perform the experiment. Two types of loading conditions were tested: an impact hammer test and a band limited excitation delivered through a shaker. The results obtained with the proposed observer are compared to the measured stress at the locations of interest, and to estimates obtained using well-established estimation methods such as Luenberger observers and the Kalman filter. The main finding is that for all experiments conducted the proposed model-based observer yielded estimates with higher or comparable accuracy to all other methods considered, with the advantage of requiring significantly less computational effort and with a more direct and transparent implementation.

Keywords:
Finite Element Models, Kalman Filter, Observers, State Estimation, Stress Estimation, Structural Health Monitoring

1. Introduction

Estimation of the stress and strain tensors at unmeasurable points in a solid or structure is a common problem encountered in many fields of science and engineering. Applications range from fatigue monitoring of structural systems [19, 10], estimation of the force through a joint in the human body [12], to estimating heart kinematics [14]. In fatigue analysis, for example, the estimated stress time histories can be used as inputs to damage functions and consequently be used to estimate the failure risk due to oscillatory loads [3]. If global system response such as accelerations at a number of locations, are measured; the objective is then to reconstruct unmeasured quantities of interest (QoI) from the available measurements and a model of the system.

State estimation methods typically fall under two categories: data interpolation methods [22, 13, 5], and methods based on control theory that explicitly account for the dynamic relationship between the measurements, measurement noise, disturbances and the QoI [21]. Traditionally, data interpolation methods provide acceptable results for situations were the QoI are governed by a number of vibration modes that is less than the number of measurements and when the analyst knows a priori which modes are dominant. Otherwise, interpolation methods typically fail to provide accurate results [2].

An alternative approach is a family of methods based on estimation and control theory, known as observers [15]. An observer is a dynamical system which serves as an estimator for the state of the system of interest, and is formulated as a feedback loop driven by a linear combination of the difference between the system output measurements and the corresponding observer response. An observer is defined as convergent if the observer's state and the system's state converge with time, i.e., the error is guaranteed to converge to zero asymptotically.

*Corresponding author
Email addresses: kerazo@uvm.edu (Kalil Erazo), eric.hernandez@uvm.edu (Eric M. Hernandez)

In observer design two cases are typically encountered: an estimate of the state is sought due to unknown initial conditions and(or) unmeasured excitations. In the case of unknown initial conditions and a continuous time system description, a convergent observer is formulated by means of shifting the poles of the observer, with respect to those of the system, towards the left of the complex plane. These types of observers are known as Luenberger observers [15]. In the case of unmeasured excitations, one of the most celebrated state estimation algorithms is the Kalman filter (KF), a recursive Bayesian estimation algorithm which allows for optimal estimation (in the Euclidean sense) of the state trajectory of a linear system on the basis of a state-space model of the system and noise-contaminated measurements [11]. The two fundamental assumptions in the KF are: (i) the system is linear and (ii) excitations and measurement noise are realizations of Gaussian random processes. In most applications, only systems with a limited number of degrees of freedom are considered, mainly due to the computational difficulties that arise when implementing the KF on high dimensional systems [18].

In addition to the computational issues, theoretical issues have also been raised related to the consistency of first order observers when applied to second order symmetric systems; especially loss of symmetry, definiteness and the fact that first order observers might yield an estimate of the state that does not correspond to the physical state sought, i.e., it does not conserve the internal consistency between certain variables, such as the fact that the estimated velocities must be derivatives of the estimated displacements. This was demonstrated by Balas [1] and Hernandez [8], who concluded that unless certain restrictions are placed on the observer formulation these inconsistencies will occur and can potentially lead to significant estimation errors. Observers that satisfy the consistency requirement are known as natural observers. It has been shown that the KF is not a natural observer for linear symmetric second order models typically used in structural dynamics [8].

In this paper various experiments are conducted to validate a natural observer developed by Hernandez [8]. The objective of the experiments is to estimate the stress time histories at arbitrary locations in a cantilever beam using noise contaminated acceleration response measurements. The proposed observer resembles the KF, but with the capability of direct implementation as a modified finite element model of the system of interest and with significantly reduced computational effort. To the best knowledge of the authors, this constitutes the first published experimental validation study regarding the use of observers to estimate stress and strain fields in structures.

The paper is laid out as follows; a brief introduction to the theory behind the proposed model-based observer (MBO) is presented in the first section. Additionally, some essential aspects of observer theory and Kalman filtering are discussed. This is followed by a section describing the laboratory experiments and the results. It is shown that the estimates from the proposed model-based observer outperform the Luenberger observer and are comparable (and sometimes superior) to the Kalman filter estimates.

2. Theoretical Background

In this paper we restrict our attention to systems whose dynamic response can be accurately described by the following matrix ordinary differential equation:

$$\mathbf{M}\ddot{q}(t) + \mathbf{C}_d\dot{q}(t) + \mathbf{K}q(t) = \mathbf{b}_1 u(t) + \mathbf{b}_2 w(t) \tag{1}$$

where $\mathbf{M} = \mathbf{M}^T > 0 \in R^{N\times N}$ is the mass matrix, $\mathbf{C}_d = \mathbf{C}_d^T > 0 \in R^{N\times N}$ is the damping matrix and $\mathbf{K} = \mathbf{K}^T > 0 \in R^{N\times N}$ is the stiffness matrix. The vector $q(t) \in R^{N\times 1}$ is the displacement vector of the N degrees of freedom, $\mathbf{b}_1 \in R^{N\times r}$ defines the spatial distribution of the excitation $u(t) \in R^{r\times 1}$ and $\mathbf{b}_2 \in R^{N\times p}$ defines the spatial distribution of the unmeasured excitation $w(t) \in R^{p\times 1}$. By defining the state vector as $x(t) = [q^T(t) \quad \dot{q}^T(t)]^T$, Eq. (1) can be written in first order form as

$$\dot{x}(t) = \mathbf{A}_c x(t) + \mathbf{B}_1 u(t) + \mathbf{B}_2 w(t) \tag{2}$$

where the matrices $\mathbf{A}_c$, $\mathbf{B}_1$ and $\mathbf{B}_2$ are defined as

$$\mathbf{A}_c = \begin{bmatrix} \mathbf{0}_{N\times N} & \mathbf{I}_{N\times N} \\ -\mathbf{M}^{-1}\mathbf{K} & -\mathbf{M}^{-1}\mathbf{C}_D \end{bmatrix} \tag{3}$$

$$\mathbf{B}_1 = \begin{bmatrix} \mathbf{0}_{N\times r} \\ \mathbf{M}^{-1}\mathbf{b}_1 \end{bmatrix} \qquad \mathbf{B}_2 = \begin{bmatrix} \mathbf{0}_{N\times p} \\ \mathbf{M}^{-1}\mathbf{b}_2 \end{bmatrix} \tag{4}$$

Feedback measurements $y(t)$ at discrete points in the structure are given by

$$y(t) = \mathbf{C}x(t) + \mathbf{D}_1 u(t) + \mathbf{D}_2 w(t) + \nu(t) \tag{5}$$

where for acceleration feedback $\mathbf{C} = \mathbf{c}_2[-\mathbf{M}^{-1}\mathbf{K} \quad -\mathbf{M}^{-1}\mathbf{C}_d]$, $\mathbf{D}_1 = \mathbf{c}_2\mathbf{M}^{-1}\mathbf{b}_1$, $\mathbf{D}_2 = \mathbf{c}_2\mathbf{M}^{-1}\mathbf{b}_2$; for displacement feedback $\mathbf{C} = [\mathbf{c}_2 \quad \mathbf{0}_{m\times N}]$ and for velocity feedback $\mathbf{C} = [\mathbf{0}_{m\times N} \quad \mathbf{c}_2]$. For displacement and velocity measurements $\mathbf{D}_1$ and $\mathbf{D}_2$ are zero matrices of appropriate dimensions. The output distribution matrix $\mathbf{c}_2 \in R^{m\times N}$ is a Boolean matrix where m is the number of measurements, and $\nu(t)$ is the measurement noise, a realization of a Gaussian random process with zero mean and known covariance matrix $\mathbf{R}(t)$.

Observability

A prerequisite for any state estimation to be successful is observability. A state $x(t_o)$ is observable if it can be determined from knowledge of the system matrices and the output $y(t)$ for $t > t_o$. If all possible states of a system are observable, then we say the system is globally observable. For linear time-invariant systems, the global observability criteria consists in showing that the observability Grammian $\mathbf{W_o}(t_f, t_o)$ defined as

$$\mathbf{W_o}(t_f, t_o) = \int_{t_o}^{t_f} e^{\mathbf{A}^T(\tau - t_o)}\mathbf{C}^T\mathbf{C}e^{\mathbf{A}(\tau - t_o)}\mathbf{C}d\tau \tag{6}$$

is full rank [4], where t_f is the final time of observations. An equivalent, and sometimes simpler way to prove observability in structural dynamics is to show that every mode shape has at least one measurement coordinate with non-zero amplitude.

State Estimators

In general, the state estimate provided by an observer can be written in first order state-space form as

$$\dot{\hat{x}}(t) = \mathbf{A}_c\hat{x}(t) + \mathbf{B}_1 u(t) + \mathbf{G}[y(t) - \mathbf{C}\hat{x}(t) - \mathbf{D}_1 u(t)] \tag{7a}$$

$$= (\mathbf{A}_c - \mathbf{GC})\hat{x}(t) + \mathbf{B}_1 u(t) + \mathbf{G}[y(t) - \mathbf{D}_1 u(t)] \tag{7b}$$

where $\hat{x}(t)$ represents an estimate of $x(t)$. As can be seen from Eq. (7a), the observer state estimate is the response of the system subject to excitations consisting of the weighted difference between measured response and model response estimates. The feedback gain matrix $\mathbf{G} \in R^{2N\times m}$ is the essence of observer design, and it is selected based on the minimization of an objective function of the state error $e(t) = x(t) - \hat{x}(t)$, where $e(t)$ is governed by the following stochastic differential equation

$$\dot{e}(t) = (\mathbf{A}_c - \mathbf{GC})e(t) + (\mathbf{B}_2 - \mathbf{GD}_2)w(t) - \mathbf{G}\nu(t) \tag{8}$$

In the continuous time Luenberger observer setting, estimation error is driven by unknown initial conditions and $w(t) = 0 \ \forall t$, and thus, the stability of the state estimation error is governed by the real-part of the eigenvalues of the matrix $\mathbf{F} = \mathbf{A}_c - \mathbf{GC}$. The matrix $\mathbf{G}$ is then selected such that $\Re(\lambda_F) < \Re(\lambda_{A_c})$ and as $\Re(\lambda_F)$ becomes more negative, the state estimation error diminishes more rapidly, but at the same time it becomes more susceptible to measurement noise and model error.

In the Kalman filter formulation it is assumed that the unmeasured excitations $w(t)$ and measurement noise $\nu(t)$ are realizations of Gaussian random processes with zero mean and covariance matrices $\mathbf{Q}(t)$ and $\mathbf{R}(t)$ respectively. The objective function is the Euclidean norm of the state error vector $\sum_i e(t)_i^2 = Tr(\mathbf{P}(t))$, where $\mathbf{P}(t)$ is the state error covariance given by the solution of

$$\dot{\mathbf{P}}(t) = \mathbf{AP}(t) + \mathbf{P}(t)\mathbf{A}^T - \mathbf{K}(t)\mathbf{R}(t)\mathbf{K}(t)^T + \mathbf{Q}(t) \tag{9}$$

where $\mathbf{K}(t)$ is given by

$$\mathbf{K}(t) = \mathbf{P}(t)\mathbf{C}^T\mathbf{R}(t)^{-1} \tag{10}$$

It can be shown that given the assumptions, selecting $\mathbf{G} = \mathbf{K}$ is the optimal choice in the sense that it minimizes the desired objective function [7].

Model-Based Observer

The proposed model-based observer is derived by rewriting Eq. (7a) in a partitioned form as

$$\begin{bmatrix} \dot{\hat{q}}(t) \\ \ddot{\hat{q}}(t) \end{bmatrix} = \begin{bmatrix} \mathbf{0}_{N\times N} & \mathbf{I}_{N\times N} \\ -\mathbf{M}^{-1}\mathbf{K} & -\mathbf{M}^{-1}\mathbf{C}_d \end{bmatrix} \begin{bmatrix} \hat{q}(t) \\ \dot{\hat{q}}(t) \end{bmatrix} + \begin{bmatrix} \mathbf{G}_1 \\ \mathbf{G}_2 \end{bmatrix} \Delta y(t) + \mathbf{B}_1 u(t) \tag{11}$$

where $\Delta y(t) = y(t) - \mathbf{C}\hat{x}(t) - \mathbf{D_1}u(t)$ is the output residual. In order for $\dot{\hat{q}}(t) = \ddot{\hat{q}}(t)$ it is necessary that $\mathbf{G}_1\Delta y(t) = 0$, which means that either $\mathbf{G}_1 = \mathbf{0}_{N\times m}$ or $\Delta y(t) \in \mathscr{N}(\mathbf{G}_1)\ \forall t$. Since the latter is not possible, the former is true and the feedback gain needs to have the form

$$\mathbf{G} = \begin{bmatrix} \mathbf{0}_{N\times m} \\ \mathbf{G}_2 \end{bmatrix} \tag{12}$$

where $\mathbf{G}_2 \in R^{N\times m}$ is still free to be selected. At this point we note that mainly three choices are available for response measurement feedback: displacement, velocity or acceleration measurements. It was shown in [8] that the best choice is velocity measurements, because as it will be seen, this retains the undamped frequencies of the system model, which will naturally reduce the estimation error. Denoting $\dot{q}_m(t)$ as measured velocities (readily obtained from acceleration measurements), the output residual is given by

$$\Delta y(t) = \dot{q}_m(t) - \mathbf{c}_2\dot{\hat{q}}(t) \tag{13}$$

and since from the form of $\mathbf{G}$ it follows that $\dot{\hat{q}}(t) = \ddot{\hat{q}}(t)$, the bottom partition of Eq. (11) becomes

$$\mathbf{M}\ddot{\hat{q}}(t) + (\mathbf{C}_D + \mathbf{M}\mathbf{G}_2\mathbf{c}_2)\dot{\hat{q}}(t) + \mathbf{K}\hat{q}(t) = \mathbf{M}\mathbf{G}_2\dot{q}_m(t) + \mathbf{b}_1 u(t) \tag{14}$$

This is a second-order matrix differential equation of the same form of Eq. (1) which represents the system of interest. The requirement for the proposed observer to be realizable as a finite element model (FEM) is that the matrix $\mathbf{M}\mathbf{G}_2\mathbf{c}_2$ must be symmetric and positive-definite, such that the resulting damping matrix retains a physical interpretation. The proposed form of the lower partition for the gain matrix is then

$$\mathbf{G}_2 = \mathbf{M}^{-1}\mathbf{c}_2^T\mathbf{E} \tag{15}$$

where $\mathbf{E} = \mathbf{E}^T \in R^{m\times m}$ remains free to be selected ($m^2 + 1 - m$ free scalars). By close examination of Eq. (14), the model-based observer can then be physically interpreted as the original system with added viscous damping $\mathbf{c}_2^T\mathbf{E}\mathbf{c}_2$ and driven by the forces $\mathbf{c}_2^T\mathbf{E}\dot{q}_m(t) + \mathbf{b}_1 u(t)$. The diagonal terms of $\mathbf{E}$ are equivalent to grounded dampers and the off-diagonal terms (typically set to zero) are equivalent to dampers connecting the respective degrees of freedom.

In order to determine the optimal value of $\mathbf{E}$, the objective function to be minimized in the proposed observer is the trace of the displacement error covariance matrix given by

$$J = tr(\mathbb{E}[(q(t) - \hat{q}(t))(q(t) - \hat{q}(t))^T]) = tr\left(\int_{-\infty}^{+\infty} \mathbf{\Phi}_{ee}(\omega)d\omega\right) \tag{16}$$

where it was shown in [8] that the estimation error power spectral density matrix is given by

$$\mathbf{\Phi}_{ee}(\omega) = \mathbf{H}_o\mathbf{b}_2\mathbf{\Phi}_{ww}(\omega)\mathbf{b}_2^T\mathbf{H}_o^* + \mathbf{H}_o\mathbf{c}_2^T\mathbf{E}\mathbf{\Phi}_{vv}(\omega)\mathbf{E}^T\mathbf{c}_2\mathbf{H}_o^* + \mathbf{H}_o\mathbf{b}_2\mathbf{\Phi}_{wv}(\omega)\mathbf{E}^T\mathbf{c}_2\mathbf{H}_o^* + \mathbf{H}_o\mathbf{c}_2^T\mathbf{\Phi}_{vw}(\omega)\mathbf{b}_2^T\mathbf{H}_o^* \tag{17}$$

and

$$\mathbf{H}_o = \left(-\mathbf{M}\omega^2 + \left(\mathbf{C}_D + \mathbf{c}_2^T\mathbf{E}\mathbf{c}_2\right)i\omega + \mathbf{K}\right)^{-1} \tag{18}$$

The matrices $\mathbf{\Phi}_{ww}$, $\mathbf{\Phi}_{vv}$, $\mathbf{\Phi}_{wv}$ and $\mathbf{\Phi}_{vw}$ are the power spectral density of the disturbance, measurement noise and cross-spectral density between the disturbance and the measurement noise. Both cross-spectral densities are zero matrices when the disturbance and measurement noise processes are uncorrelated, and one of them is zero mean.

Note that in a similar fashion to the KF, the matrix $\mathbf{E}$ is selected to minimize the trace of the estimation error covariance matrix. However the difference is that in the KF the objective function corresponds to the trace of the full state error covariance matrix which includes quantities of different units (displacement and velocity). In the proposed observer only the trace of the displacement error covariance is minimized. Given the direct relationship between

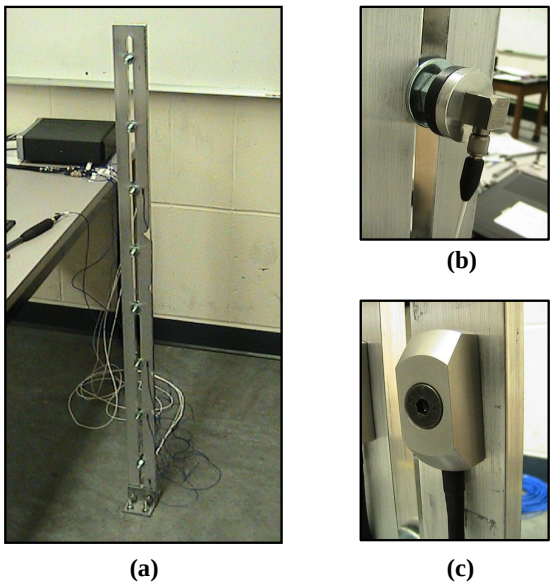

Figure 1: Experimental setup for modal hammer test; **(a)** Instrumented test beam, **(b)** Accelerometer, **(c)** Strain sensor.

displacement and velocity, minimization of velocity error is implied and guaranteed. Additional information on the derivation of the proposed MBO can be found in [8, 9].

Finally, the estimate for stress time histories $\sigma(t)$ are obtained by the linear transformation

$$\hat{\sigma}(t) = \mathbf{T}\hat{q}(t) \tag{19}$$

where $\mathbf{T}$ maps the estimated displacement field to the stress field. In the case of the proposed model-based observer $\mathbf{T}$ does not need to be computed explicitly. The stress calculation is done directly within the finite element model framework. In the case of the Luenberger observer and Kalman filter the matrix $\mathbf{T}$ needs to be computed explicitly.

3. Experiment and Procedure

An instrumented aluminum cantilever beam (Fig.1) with dimensions as shown in Fig. 2a, was used to conduct the experiment validation. Based on free vibration data, the fundamental vibration mode of the beam was identified with a frequency of 6.4 Hz and a damping ratio of approximately 0.0045.

The cantilever is instrumented with three accelerometers (PCB 333B30), two strain sensors (PCB 740B02), and a force sensor (PCBC02) located at the rod connecting the shaker and the structure. A photograph of the instrumented beam is shown in Fig. 1 and Fig. 2b. The data was recorded using the LMS Scadas Mobile Data Acquisition System at a sampling frequency of 16,384 Hz. The experimental set-up is shown in Fig. 2a where the applied load locations, strain measurements and accelerometer measurements positions are indicated.

The objective is to estimate the longitudinal stress time histories at positions (1) and (4), using the acceleration measurements at positions (3) and (9). Two loading conditions were considered: (i) an impact load generated using a modal hammer (PCB086C03) and (ii) a random load generated using an electrodynamic shaker (TMS2060E). The modal hammer excitations were separately applied at positions (3) and (9). The shaker generated load was applied at position (8) (See Fig. 2a). The position of the accelerometers was selected by maximizing the system observability via Eq. (6).

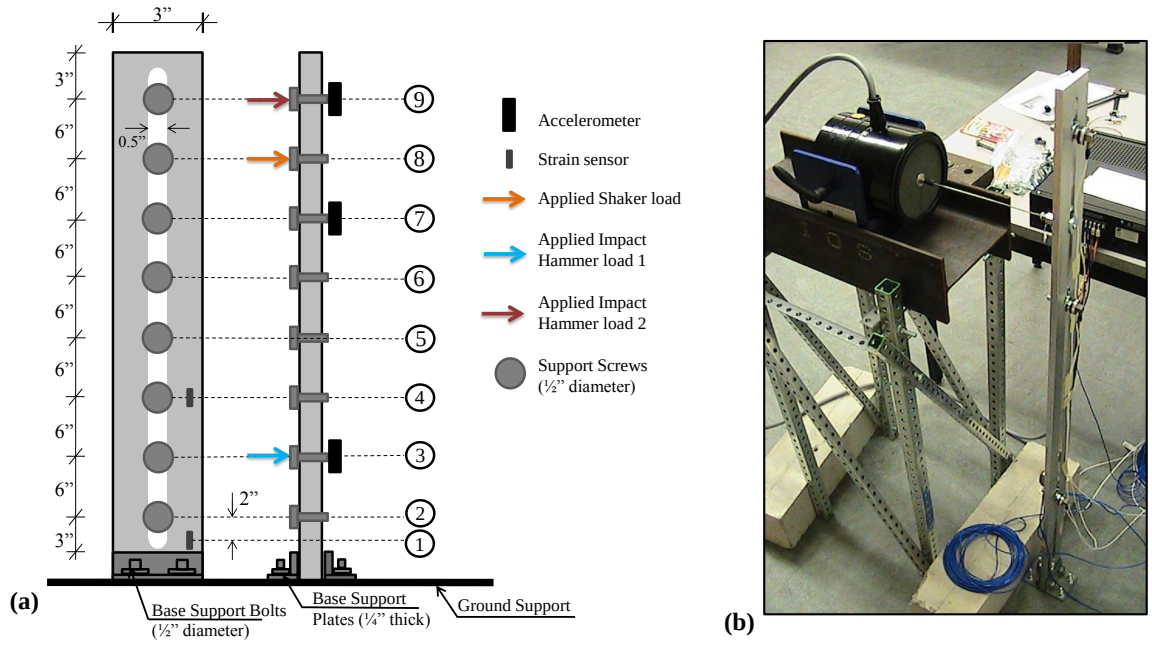

Figure 2: **(a)** Cantilever test beam with indicated dimensions, location for loads, and sensor measurements, **(b)** Experimental set-up for electrodynamic shaker test.

The estimates obtained with the proposed observer will be compared to the measured response (assumed unmeasured for the validation process) and with other estimation methods. Specifically, the response estimated from the modal impact hammer will be compared to the estimate obtained using a Luenberger observer formulated using a pole placement algorithm. For the shaker loading condition, a Kalman filter estimate was used for comparison purposes.

Model-Based Observer Formulation

To implement the proposed observer we begin by setting a FEM of the system and proceed to minimize Eq. (16) to determine the optimal value of the matrix $\mathbf{E}$. For this purpose, a surrogate model is used to perform the optimization, and a refined FEM model is then used to implement the proposed observer. For this validation study, Fig. 4(a) shows the FEM used to formulate and solve Eq. (16), while Fig. 4(b) presents the more refined FEM used to actually implement the observer. The frame element model shown in Fig. 4(a) contains 16 frame elements and 32 degrees of freedom (DoF) (axial DoF were condensed), while the more refined model shown in Fig. 4(b) was formulated using 477 shell elements and 11,448 DoF (24 DoF per element, 6 DoF per node). The fundamental frequencies for the simplified and refined FEM are 6.52 Hz and 6.37 Hz respectively. Note that the added dampers and driving forces are the same for both models and thus the proposed methodology allows for the flexibility of increasing or refining the model resolution without having to solve for the feedback gain repeatedly on increasingly larger and more refined models. This dramatically reduces the computational cost necessary to implement the proposed MBO with respect to the KF.

To perform the optimization of Eq. (16) the power spectral density (PSD) of the load and noise processes are required. The PSD of the applied load was estimated using the Bartlett method of averaging periodograms [20]. For this purpose, a shaker generated discrete time signal consisting of 917,500 points was subdivided into 100 sequences of 9,175 points each. For each segment, the periodogram is computed using the Discrete Fourier Transform of the sequence, and then the PSD estimate at a given frequency is given by the average of the periodograms at that frequency. The estimated load PSD is shown in Fig. 5. The measurement noise PSD was estimated at $\Phi_{vv} = 2.25 \times 10^{-6} I_{2\times 2}$. This value is based on an equivalent constant PSD found using the sensor measurement noise variance provided by the sensors manufacturer.

It is worth to emphasize that the PSD of the load delivered through the shaker is significantly different from constant in the 0 to 300 Hz range input specified in the shaker software. This is chiefly due to the dynamic interaction

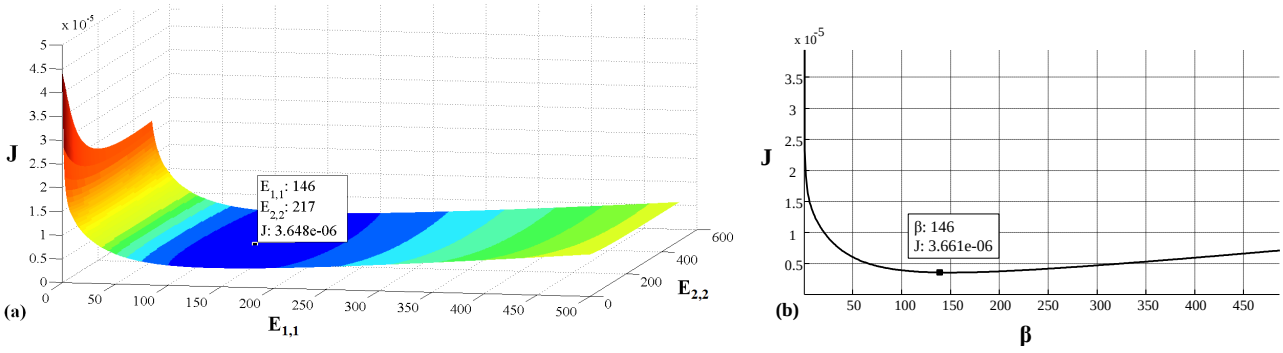

Figure 3: Optimization Results; **(a)** 2D Optimization, **(b)** 1D Optimization.

between the shaker, the platform and the cantilever beam.

The optimization problem defined by minimizing Eq. (16) can be re-written as

$$\beta_i^* = \underset{\beta_i \in R}{\arg\min} \quad tr(\mathbb{E}[(q(t)-\hat{q}(t))(q(t)-\hat{q}(t))^T]) \tag{20}$$

where $\mathbf{E}$ is diagonal and $\mathbf{E}_{i,i} = \beta_i \in R$, and β_i^* denote the optimal values. The results of the 2-dimensional optimization are shown in Fig. 3(a). The optimal point is found at $(E_{1,1}, E_{2,2}) = (146, 217)$ and the corresponding value of the objective function is $J = 3.648 \times 10^{-6}$. The optimization problem can be simplified using the parametrization $E = \beta I_{m\times m}$, where $\beta \in R$. This simplification reduces the optimization to a 1-dimensional problem, and the results are shown in Fig. 3(b), where the optimal value is found at $\beta = 146$ and the value of the objective function is $J = 3.661 \times 10^{-6}$. As it can be seen, the difference between the 1-D and the 2-D optimization is negligible; mainly because the damper at DoF 16 (Fig. 4(a)) controls the optimization. This is clearly shown in Fig. 3(a) where we can appreciate the dependence of the objective function with respect to each damper.

It is worth noting that for higher dimensions, efficient numerical optimization algorithms can be used to solve the optimization problem. For example, the authors have used random walks constructed using Markov chain Monte Carlo (MCMC) algorithms to generate samples from the parameter space formed by the vectors $[\beta_1 \quad \beta_2 \quad \dots \quad \beta_N]^T \in R^N$. In this setting, methods like the Metropolis algorithm can be viewed as a stochastic version of a stepwise mode finding algorithm, where the "density function" is the observer objective function [6].

Kalman filter Formulation

To formulate a discrete-time Kalman filter for this problem three matrices are necessary: the covariance matrix of the initial condition error, the measurement noise covariance and the disturbance covariance matrix [7]. We selected the initial state error covariance matrix as zero since we are starting the experiment with the structure at rest. It was shown [7] that the noise and disturbance covariance matrices in discrete time can be approximated as a function of the continuous matrices as

$$R = R_o/\Delta t \tag{21}$$

$$Q = \int_0^{\Delta t} e^{A_c \Delta t} B_1 Q_o B_1^T (e^{A_c \Delta t})^T dt \approx B_1 Q_o B_1^T \Delta t \tag{22}$$

where for the present experiment $R_o = 2.25 \times 10^{-6} I_{2\times 2}\delta_o$ and $Q_o = 950.5\delta_o$ are the continuous noise and disturbance correlation matrices for the equivalent Gaussian white processes, δ_o is the Dirac delta function at the origin.

As mentioned previously, these are nominal values computed based on sensor information and input values through the shaker software. As can be seen from Fig. 5, the equivalent white process of the unmeasured excitation description differs from that of the actual load process applied to the structure, and thus issues regarding robustness in the processes description are important and cannot be neglected. It is worth noting that due to the computational burden, the KF could only be implemented using the frame model of Fig. 4(a). We will return to this issue when we discuss the computational cost required by the algorithms in the results section of this paper.

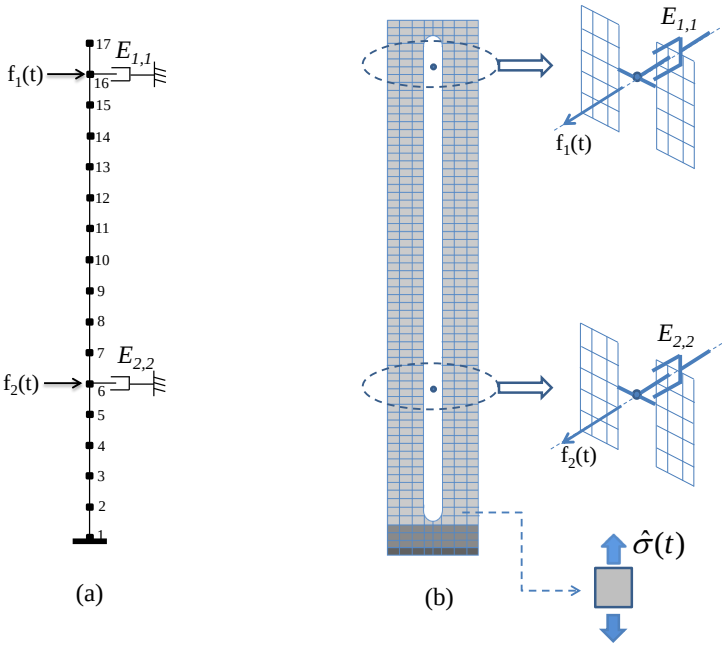

Figure 4: **(a)** FEM used to perform the minimization (16 frame elements), **(b)** FEM used to perform the estimation (477 shell elements).

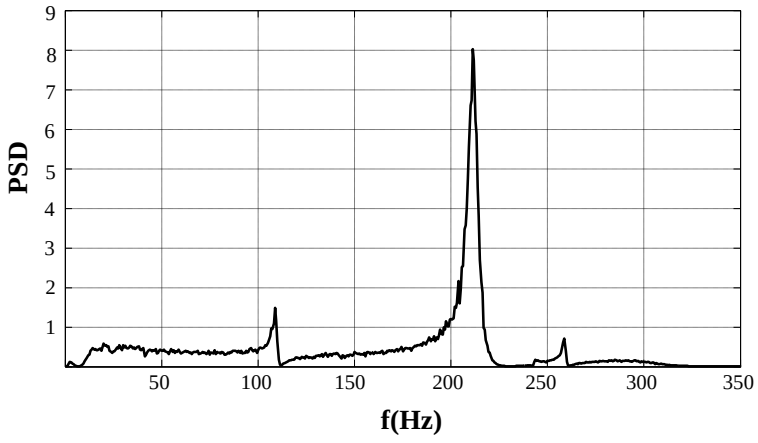

Figure 5: Estimated power spectral density of shaker induced load process. Computed using the Bartlett method with 100 averages.

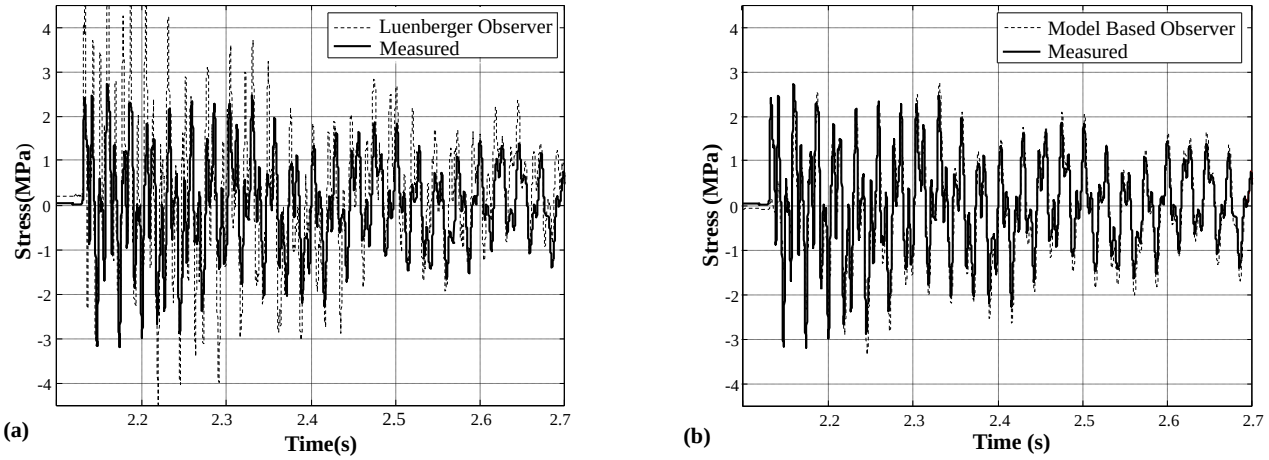

Figure 6: Stress at position (1); **(a)** measured stress vs. Luenberger estimate, **(b)** measured stress vs. MBO estimate. Hammer impact applied at position (3).

Luenberger Observer Formulation

In the case of the Luenberger observer, the only information needed is the desired position of the poles of the closed loop system $\mathbf{A}_c - \mathbf{GC}$, which needs to be in a stable region (the left complex plane for the continuous time formulation and inside the unit circle for the discrete time formulation). The pole placement can be achieved only if the model is globally observable at the measurement locations. This is a sufficient condition for the state error vector to go asymptotically to zero.

For this experiment a Luenberger observer in discrete time was implemented by setting $\|\lambda_{cl}\| = 0.95\|\lambda_{ol}\|$ and $\angle\lambda_{cl} = \angle\lambda_{ol}$; where λ_{cl} are the poles of the closed loop system in discrete time formulation and λ_{ol} are poles of the open loop system (the FEM model of the beam shown in Fig. 4(a)) in discrete time formulation. The algorithm used to achieve the pole placement was the one proposed in [4]. Note that the closer the poles of the closed loop system are to the origin, the faster the estimate will converge to the true state, however the more sensitive the observer becomes to measurement noise and model error. Additionally, whenever the desired poles locations are too close to each other the pole placement algorithm becomes unstable and cannot place the poles at the desired location. The selected value of 0.95 was based on the maximum capability of the pole placement algorithm to place the poles. Finally, since we are using constant modal damping, all poles of the closed loop system will lie on a circle centred at the origin in the complex plane [17].

4. Results and Discussion

In this section we present and discuss the results of the various experiments carried out and display the comparison between the accuracy of the various state estimation algorithms. In all the comparisons we converted the measured strain to stress by multiplying strain by the elastic modulus of aluminum ($E_{Al} = 69$ GPa).

4.1. Impact Hammer Test

In this section we present the experimental results corresponding to the case of unknown initial conditions delivered through an impact hammer. For this purpose, the results from the proposed observer are compared to those obtained through a Luenberger observer formulated as described in the previous section. Fig. 6 presents a representative time lapse comparison between the measured stress and estimated stress at position (1) for the case of an impact load applied at location (3) (see Fig. 2a). We can appreciate that the Luenberger observer displays some tracking capability, but the noise amplification is evident. The proposed model-based observer outperforms the Luenberger observer estimate both in the estimation of maximum response and in overall tracking capabilities.

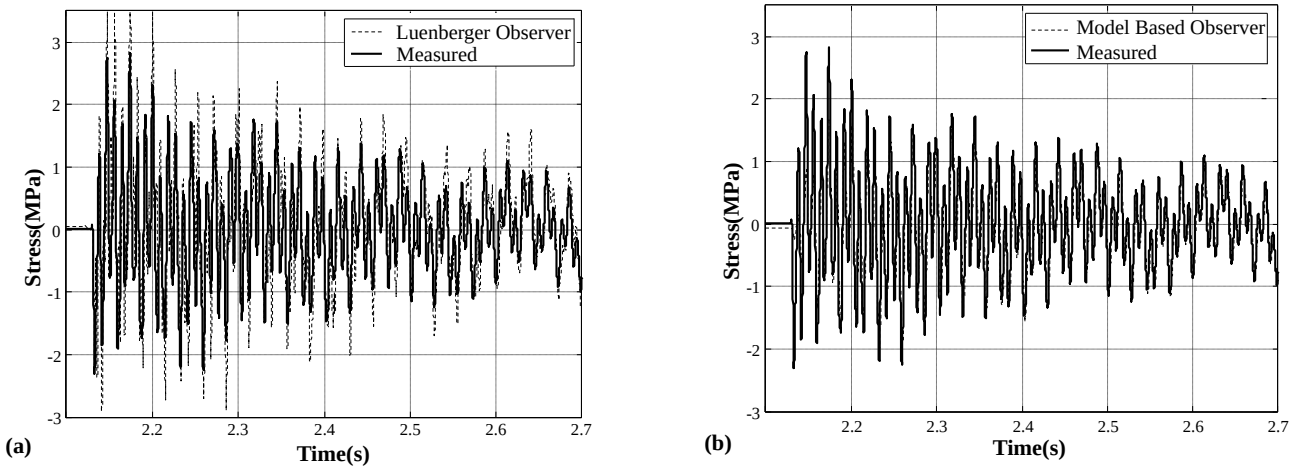

Figure 7: Stress at position (4);**(a)** measured stress vs. Luenberger estimate, **(b)** measured stress vs. MBO estimate. Hammer impact applied at position (3).

Fig. 7 shows a comparison between the measured stress and estimated stress at position (4). In this case the impact was applied at location (3) (see Fig. 2a). As in the previous case, significant improvements in estimation are obtained with the proposed MBO.

Fig. 8 and Fig. 9 present a similar comparison with the impact applied at location (9) (see Fig. 2a).

4.2. Shaker Test

In this section we present the experimental results corresponding to the case where the test structure is excited by a realization of a stochastic process with known power spectral density given by Fig. 5. The results of the model-based observer will be compared with those obtained by formulating a Kalman filter. The specific realization of the load process that generated the data used for this experiment is shown in Fig.11.

Fig. 10 shows a comparison between the measured stress and estimated stress at position (1) using a Kalman filter and the proposed model-based observer. As can be seen, the proposed observer has similar tracking capabilities to the KF. Fig. 12 presents a comparison between the measured stress and estimated stress at position (4) using a Kalman filter and the proposed model-based observer, for the same loading conditions described before. As in the previous case, both estimates are of comparable accuracy, however, the model-based observer provides improvement in tracking the peak amplitude in each cycle. This partly explains its advantage in estimating the number of upcrossings more accurately in an important region of threshold values. This is clearly shown in Fig. 14.

The MBO stress contour estimate at $t = 6.6s$ is shown in Fig. 13. As stated before, an important advantage of the proposed MBO is that response quantities that are cumbersome transformations of the state of the system are directly available through the FEM.

The computational time required to implement the proposed model-based observer using a commercial FEM software was 22 seconds. In order to implement the Kalman filter in the refined model, the mass and stiffness matrices were extracted from the FEM software and the conventional Kalman filter algorithm was implemented using Matlab [16]. Every step of the Kalman filter (state prediction and correction steps) takes approximately 520 seconds, and since our data involves 41,448 steps, it would take around 250 days to run the KF in the refined model, which is clearly impractical. Both algorithms were run on a computer with an Intel i7 2.93GHz processor and 16GB RAM memory.

The two main computational challenges faced in applying the KF in high-dimensional systems were: (i) the propagation of the covariance matrix, governed by an algebraic Ricatti equation [7], and (ii) the required matrix inversion of the measurement error covariance matrix. The comparison of the required computational time shows that it is impractical to implement the standard KF formulation in FEM with a large number of DoF's ($\mathcal{O}10^4$). The

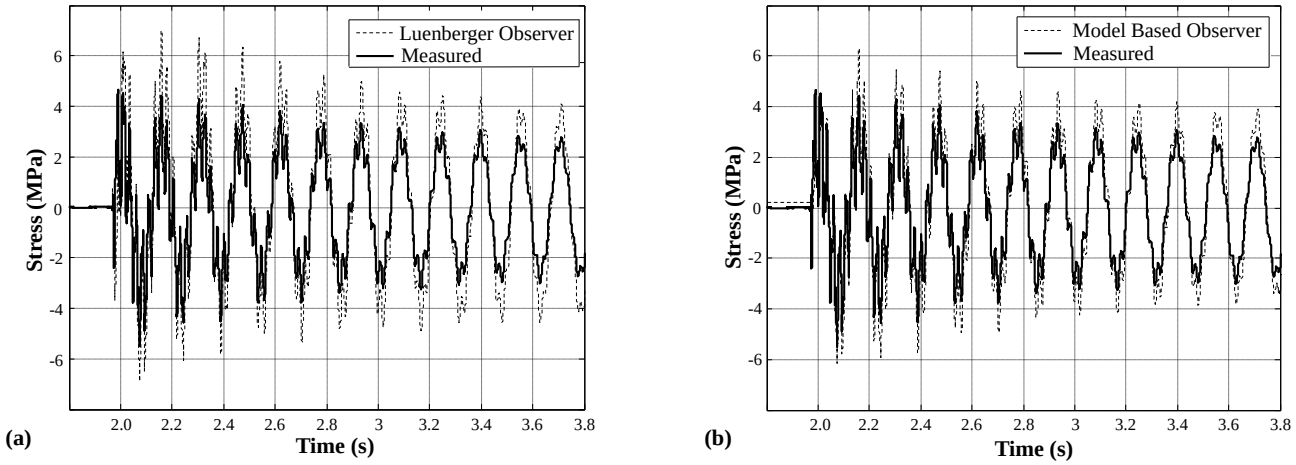

Figure 8: Stress at position (1); **(a)** measured stress vs. Luenberger estimate, **(b)** measured stress vs. MBO estimate. Hammer impact applied at position (9).

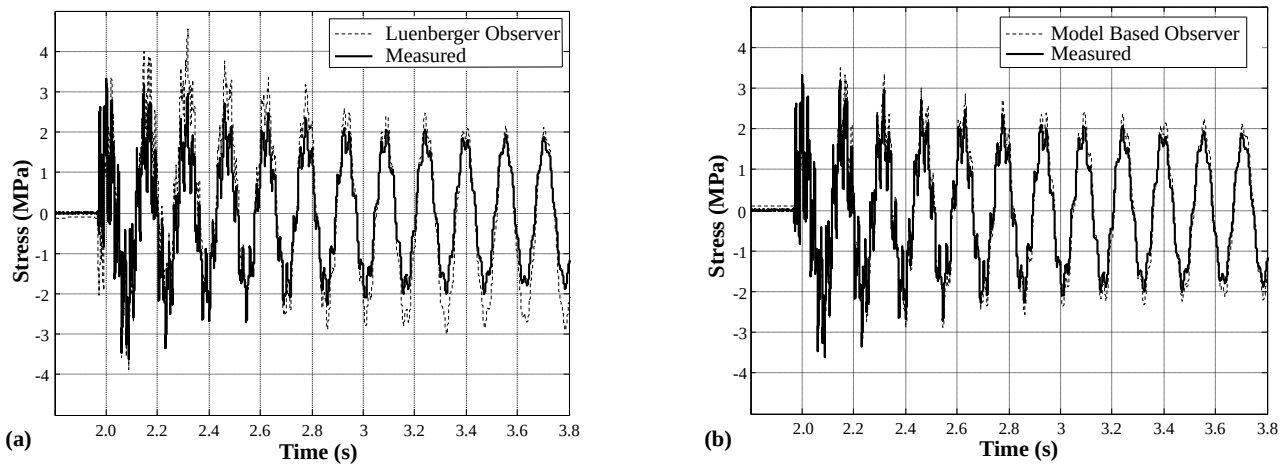

Figure 9: Stress at position (4); **(a)** measured stress vs. Luenberger estimate, **(b)** measured stress vs. MBO estimate. Hammer impact applied at position (9).

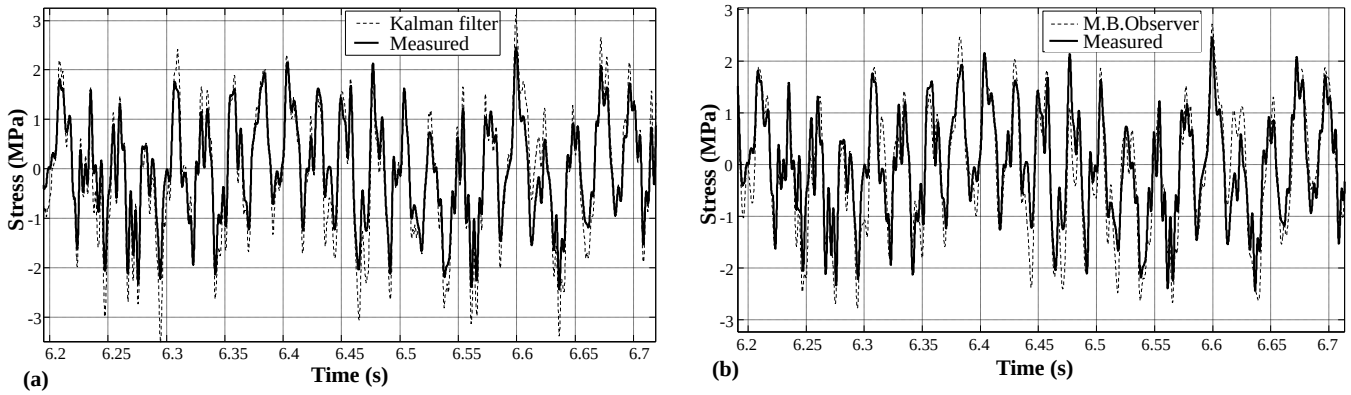

Figure 10: Stress at position (1); **(a)** measured stress vs. Kalman filter estimate, **(b)** measured stress vs. MBO estimate. Shaker load applied at position (8).

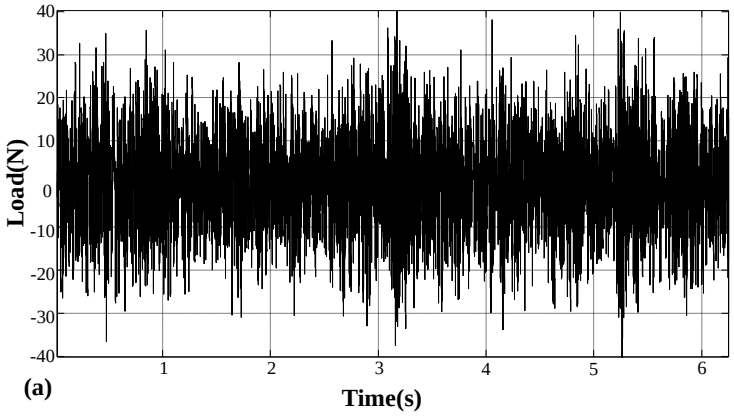

Figure 11: Realization of the load process that generated the experiment data.

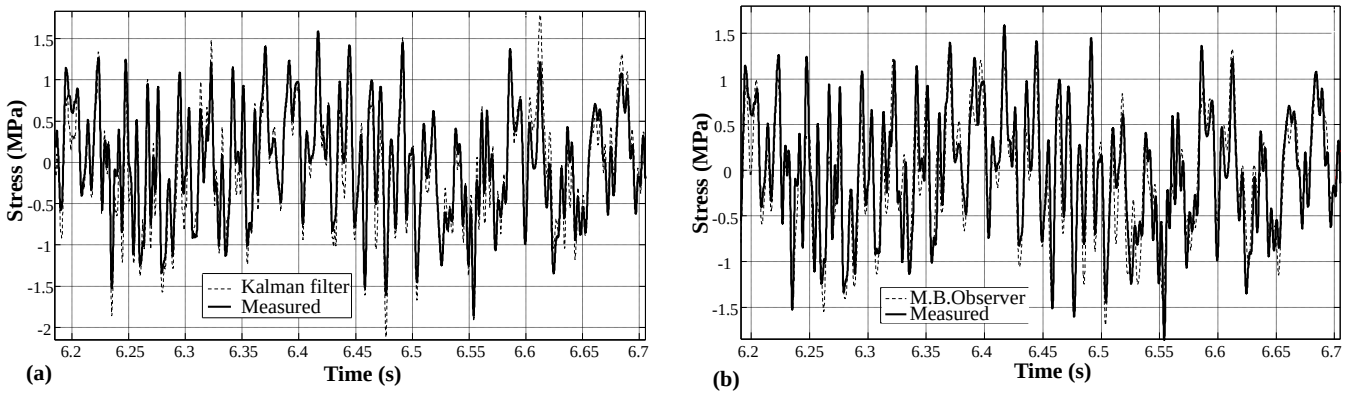

Figure 12: Stress at position (4); **(a)** measured stress vs. Kalman filter estimate, **(b)** measured stress vs. MBO estimate. Shaker load applied at position (8).

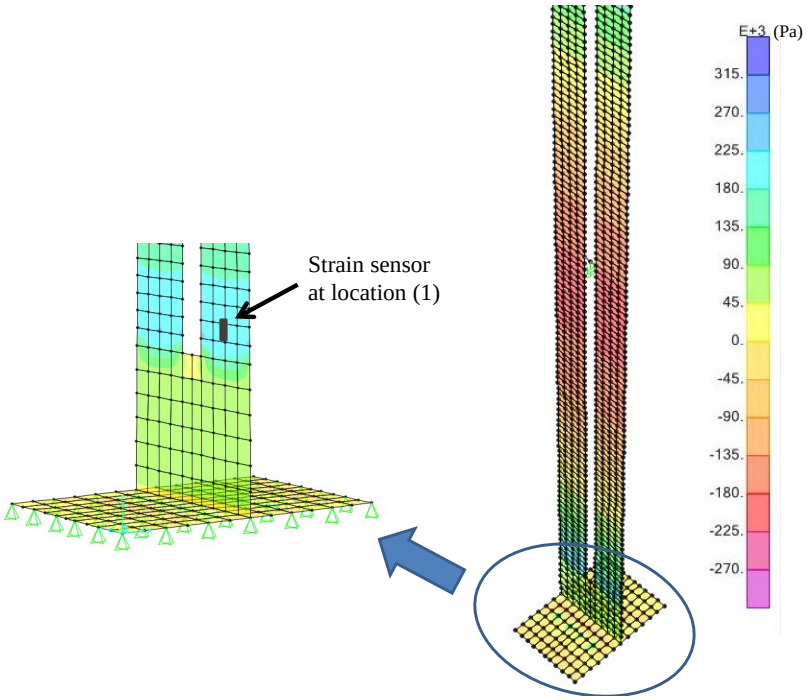

Figure 13: MBO stress contour estimate at $t = 6.6s$.

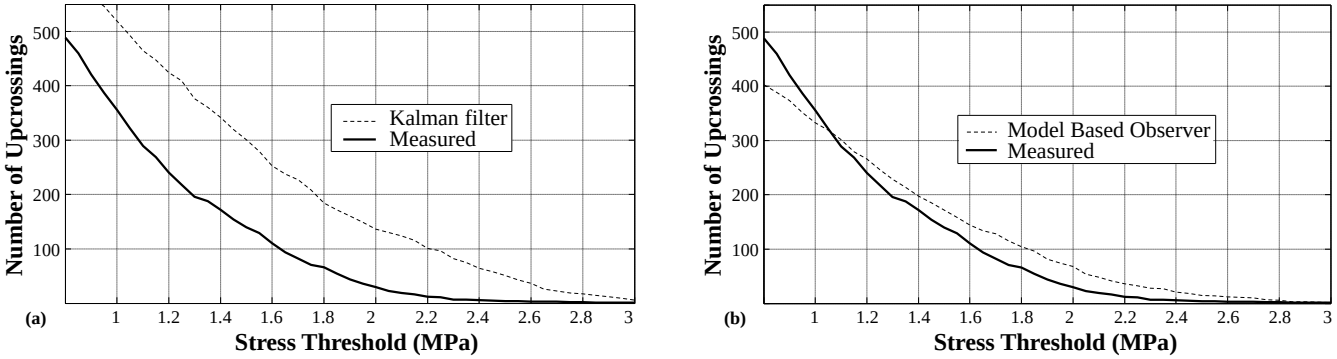

Figure 14: Estimated number of upcrossings; **(a)** measured stress vs. Kalman filter estimate, **(b)** measured stress vs. MBO estimate.

proposed MBO exploits the mathematical structure of second order systems and the capability of FEM software solvers to perform the estimation without significant loss of accuracy with respect to the KF, but with an important reduction in computational effort.

5. Conclusion

The paper presents an experimental validation study of a model-based observer previously proposed by one of the authors. The study was conducted using an instrumented aluminum cantilever beam. The proposed observer was implemented as a modified finite element model of the system of interest, subjected to corrective forces proportional to the measurements. It was shown that the overall tracking accuracy of the proposed estimator exceeds that of the Luenberger observer, and is comparable to the Kalman filter, with significant improvement in the higher amplitude region of the stress cycles. This provides a better estimate of the expected number of upcrossings for a wide range of stress values.

It was also shown that whenever a high fidelity finite element model is used, dramatic computational gains can be obtained (without appreciable loss of accuracy) with the proposed observer in comparison with the Kalman filter. This is possible because the feedback matrix of the proposed observer has a physical meaning and can be computed using a low dimensional model and subsequently applied to a more refined topologically consistent model, without the need to recompute it.

References

[1] MJ Balas. Do all linear flexible structures have convergent second-order observers?. *AIAA J Guidance, Control and Dynamics*, 4:23192323, 1998.

[2] D Bernal and A Nasseri. Schemes for reconstructing the seismic response of instrumented buildings. *SMIP Seminar on Seismological and Engineering Implications of Recent Strong Motion Data*, 23-38, 2009.

[3] V Bolotin. *Mechanics of Fatigue*. CRC Press, Boca Raton, FL, USA, 1999.

[4] W Brogan. *Modern Control Theory*. Prentice Hall, New Jersey, USA, 1991.

[5] C Chipman and P Avitable. Expansion of transient operating data. *Mechanical Systems Signal Processing*, 31:112, 2012.

[6] A Gelman, J Carlin, H Stern, and D Rubin. *Bayesian Data Analysis*. Chapman and Hall/CRC, Boca Raton, Florida, USA, 2004.

[7] M Grewal and A Andrews. *Kalman Filtering, Theory and Practice using MATLAB*. Wiley, New Jersey, USA, 1998.

[8] EM Hernandez. A natural observer for optimal state estimation in second order linear structural systems. *Mechanical Systems and Signal Processing*, 25:29382947, 2011.

[9] EM Hernandez. Optimal model-based state estimation in mechanical and structural systems. *J Structural Control Health Monitoring*, 20:532543, 2011.

[10] EM Hernandez, D Bernal, and L Caracoglia. On-line monitoring of wind induced stresses and fatigue damage in instrumented structures. *J Structural Control Health Monitoring*, DOI: 10.1002/stc.1536, 2012.

[11] RE Kalman. A new approach to linear filtering and prediction problem. *J Basic Engineering, Trans ASME*, 82:3545, 1960.
[12] Z Ladin and G Hu. Combining position and acceleration measurements for joint force estimation. *J Biomechanics*, 24:11731187, 1991.
[13] MP Limongelli. Optimal location of sensors for reconstruction of seismic responses through spline function interpolation. *J Earthquake Engineering Structural Dynamics*, 32(1):10551074, 2003.
[14] H Liu. State-Space Analysis of Cardiac Motion With Biomechanical Constraints. *IEEE Trans Image Process*, 16(4):901917, 2007.
[15] D Luenberger. *Observer Theory*. John Wiley and Sons, New York, NY, USA, 1970.
[16] MATLAB. The MathWorks Inc., Massachusetts, USA, R2012a.
[17] L Meirovitch. *Fundamentals of Vibrations*. McGrawHill, New York, NY, USA, 2001.
[18] J Mendel. Computational requirements for a discrete Kalman filter. *IEEE Trans Automatic Control*, 16(6):748758, 1971.
[19] C Papadimitriou, CP Fritzen, P Kraemer, and E Ntotsios. Fatigue predictions in entire body of metallic structures from a limited number of vibration sensors using Kalman filtering. *J Structural Control and Health Monitoring*, 18(5):554573, 2011.
[20] J Proakis and D Manolakis. *Digital Signal Processing*. Prentice Hall, New Jersey, USA, 1996.
[21] D Simon. *Optimal State Estimation*. John Wiley and Sons. New York, NY, USA, 2006.
[22] L Threfeten. *Approximation Theory and Approximation Practice*. SIAM Press, USA, 2012.